This is a repository copy of *Density Functional Theory calculations on copper-mediated peroxide decomposition reactions. Implications for jet fuel autoxidation*.

White Rose Research Online URL for this paper:
https://eprints.whiterose.ac.uk/161453/

Version: Accepted Version

Article:

Parks, C.M. orcid.org/0000-0001-8016-474X, Alborzi, E. orcid.org/0000-0002-2585-0824, Blakey, S.G. et al. (2 more authors) (2020) Density Functional Theory calculations on copper-mediated peroxide decomposition reactions. Implications for jet fuel autoxidation. Energy & Fuels, 34 (6). pp. 7439-7447. ISSN 0887-0624

https://doi.org/10.1021/acs.energyfuels.0c00918

This document is the Accepted Manuscript version of a Published Work that appeared in final form in Energy and Fuels, copyright © American Chemical Society after peer review and technical editing by the publisher. To access the final edited and published work see https://doi.org/10.1021/acs.energyfuels.0c00918

Reuse

Items deposited in White Rose Research Online are protected by copyright, with all rights reserved unless indicated otherwise. They may be downloaded and/or printed for private study, or other acts as permitted by national copyright laws. The publisher or other rights holders may allow further reproduction and re-use of the full text version. This is indicated by the licence information on the White Rose Research Online record for the item.

Takedown

If you consider content in White Rose Research Online to be in breach of UK law, please notify us by emailing eprints@whiterose.ac.uk including the URL of the record and the reason for the withdrawal request.

eprints@whiterose.ac.uk
https://eprints.whiterose.ac.uk/

energy&fuels

Subscriber access provided by The University Library | University of Sheffield

Catalysis and Kinetics

Density Functional Theory calculations on copper-mediated peroxide decomposition reactions. Implications for jet fuel autoxidation

Christopher M. Parks, Ehsan Alborzi, Simon G. Blakey,
Anthony J. H. M. Meijer, and Mohammed Pourkashanian

Energy Fuels, **Just Accepted Manuscript** • DOI: 10.1021/acs.energyfuels.0c00918 • Publication Date (Web): 26 May 2020

Downloaded from pubs.acs.org on June 2, 2020

Just Accepted

"Just Accepted" manuscripts have been peer-reviewed and accepted for publication. They are posted online prior to technical editing, formatting for publication and author proofing. The American Chemical Society provides "Just Accepted" as a service to the research community to expedite the dissemination of scientific material as soon as possible after acceptance. "Just Accepted" manuscripts appear in full in PDF format accompanied by an HTML abstract. "Just Accepted" manuscripts have been fully peer reviewed, but should not be considered the official version of record. They are citable by the Digital Object Identifier (DOI®). "Just Accepted" is an optional service offered to authors. Therefore, the "Just Accepted" Web site may not include all articles that will be published in the journal. After a manuscript is technically edited and formatted, it will be removed from the "Just Accepted" Web site and published as an ASAP article. Note that technical editing may introduce minor changes to the manuscript text and/or graphics which could affect content, and all legal disclaimers and ethical guidelines that apply to the journal pertain. ACS cannot be held responsible for errors or consequences arising from the use of information contained in these "Just Accepted" manuscripts.

is published by the American Chemical Society. 1155 Sixteenth Street N.W.,
Washington, DC 20036

Published by American Chemical Society. Copyright © American Chemical Society.
However, no copyright claim is made to original U.S. Government works, or works produced by employees of any Commonwealth realm Crown government in the course of their duties.

Density Functional Theory calculations on copper-mediated peroxide decomposition reactions. Implications for jet fuel autoxidation.

Christopher. Parks, [a], Ehsan. Alborzi, [a] Simon. Blakey, [b] Anthony Meijer [c]

Mohamed. Pourkashanian, [a]

[a] Department of Mechanical Engineering, The University of Sheffield, Sheffield S3 7RD,UK

[b]Department of Mechanical Engineering, The University of Birmingham, Birmingham B15 2TT, U.K.

[c]Department of Chemistry, The University of Sheffield, Sheffield, S3 7HF

E-mail: c.m.parks@sheffield.ac.uk, e.alborzi@sheffield.ac.uk, S.G.Blakey@bham.ac.uk

a.meijer@sheffield.ac.uk

Abstract

The presence of metal impurities in jet fuel can lead to a reduction in the thermal stability of the fuel. Density Functional Theory (DFT) calculations are reported on the reactions of hydroperoxides with both bare Cu(I) ions and Cu(Naphthenate). The reaction of Cu(Naphthenate) and cumene hydroperoxide forms one product complex. Release of alkoxy radicals ($RO^\bullet$) from the product complex is energetically feasible. This provides a low energy route to radical formation when compared to hydroperoxide fission. The reaction mechanisms reported here for the copper-catalyzed hydroperoxide decomposition can be used to improve current chemical kinetic models for fuel autoxidation.

1. Introduction

Jet fuel is obviously used to propel aircraft. However, it is also exploited as a coolant in modern engines prior to being combusted. This reduces the necessity for further cooling systems which increase aircraft payload. However, this heating thermally stresses the fuel. When the fuel temperature reaches around 140 ^{O}C an autoxidation chain mechanism is initiated. At that temperature, the fuel undergoes a series of chemical reactions, which leads to the formation of surface deposits and other bulk insoluble products. These products are mainly composed of carbon, sulfur, hydrogen and nitrogen and their presence can inhibit the correct functioning of the engine by blocking filters and nozzles.[1] It has been shown experimentally that sulphides and disulphides[2, 3], polar nitrogen species[4-8], phenolic species[9, 10], dissolved metals[11-13] and hydroperoxides collectively play significant roles in the formation of these deposits.

A simplified autoxidation scheme is outlined in Figure 1 showing the schematic reactions of the main species involved. Autoxidation has been studied in depth for single component model fuels with long carbon chain lengths (C_{10} to C_{12}) [14-16]. These studies demonstrate that the autoxidation cycle proceeds through a radical chain mechanism as in Reactions 1-4 initiated by the formation of an alkyl radical species. (Reaction 1) [14-17] It is noted that this initiation step is poorly understood currently with no clear consensus on how the radicals are formed in the first instance. Reaction 2 details a propagation step. Here, the generated alkyl radical ($R^{\bullet}$) reacts with dissolved oxygen (O_2 levels are generally in the region of 65-70 ppm in fuels) to form peroxy-radicals ($RO_2^{\bullet}$) These radicals can subsequently react with RH to form a peroxide species (ROOH) and generate another alkyl radical (Reaction 3).

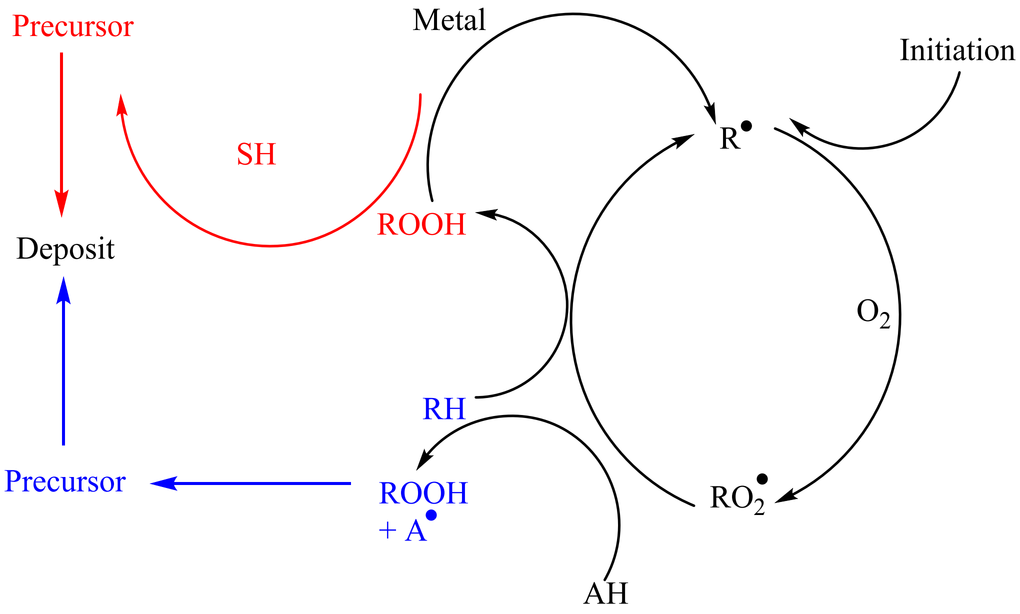

Figure 1. A simplified autoxidation scheme of liquid hydrocarbons highlighting potential routes to deposit formation *via* sulphurs (SH) and peroxides (ROOH) [12]

$$\mathrm{RH} \longrightarrow \mathrm{R}^{\bullet} \tag{1}$$

$$\mathrm{R}^{\bullet} + \mathrm{O_2} \longrightarrow \mathrm{RO_2}^{\bullet} \tag{2}$$

$$\mathrm{RO_2}^{\bullet} + \mathrm{RH} \longrightarrow \mathrm{ROOH} + \mathrm{R}^{\bullet} \tag{3}$$

$$\mathrm{ROOH} \longrightarrow \mathrm{RO}^{\bullet} + \mathrm{HO}^{\bullet} \tag{4}$$

Hydroperoxides play an important role in the autoxidation mechanism. They are found in micro-molar concentrations in jet fuel during storage. Moreover, larger quantities can also be produced during the cycle, *via* the reaction of dissolved oxygen with paraffins.[12] Hydroperoxides thermally break down at autoxidation temperatures in a barrierless process according to Reaction 4. Peroxide fission is generally quoted at 40-45 kcal mol^{-}

[1]. [18] This breakdown reaction forms two radical species, HO• and RO•, which accelerate the propagation steps. These radicals can also react with other components of the fuel, for example sulfides and disulfides which can go onto form precursors to deposits.[15, 19]

The breakdown of hydroperoxide species in fuels can be accelerated by the interaction with dissolved metals such as copper, iron, zinc and manganese. Whilst these metals have low solubility in fuel and are only present in trace quantities, it is possible that they react with dissolved organics, particularly naphthenic acids, to form fuel soluble metal naphthenates.[11] To date, the underlying nature of the interactions between dissolved metals and hydroperoxides in fuels is not clearly understood. It is therefore clear that a better understanding of the underlying mechanism of metal intervention in fuel autoxidation is critical for improving the longevity and stability of future jet fuels.

$$\mathrm{ROOH} + \mathrm{M}^{n+} \longrightarrow \mathrm{RO}^{\bullet} + \mathrm{OH}^{-} + \mathrm{M}^{(n+1)+}$$

(5)

$$\mathrm{ROOH} + \mathrm{M}^{(n+1)+} \longrightarrow \mathrm{ROO}^{\bullet} + \mathrm{H}^{+} + \mathrm{M}^{n+} \qquad (6)$$

The mechanism of hydroperoxide decomposition by metals is often cited as a two-step redox process as in Reaction 5 and Reaction 6.[20, 21] The reaction is first initiated by the formation of a metal-peroxide complex which then undergoes electron transfer to form radicals. If the metal is a strong reducing agent, the first reaction dominates. On the other hand if the metal is a strong oxidizing agent then the second reaction dominates. This two-step process in biology is referred to as the Fenton reaction.[22] The largest effect on fuel stability is observed when the metal can act as both a reducing and oxidizing agent as is the case with copper.

Historically, the negative effect of metals on deposit formation was first observed by Bridgeman in 1932. In his experiments the presence of trace metals caused more gum formation. [23] In 1949, Peterson *et al*. showed a copper concentration of 1 ppm required the use of four equivalents of antioxidant to achieve the same level of autoxidation resistance as in the absence of copper.[24] This illustrates that copper can retain activity even in the presence of significant excess antioxidant species.

More recently, a computational study into the effect that copper can have on hydroperoxide decomposition was reported by Zabarnick and co-workers.[25] In their work they used the B3LYP[26-28] functional and the 6-31G(d,p) basis set. Initially, the peroxide (1-phenylethyl hydroperoxide in this case) was found to bind favorably with a Cu(II) ion through the hydroxyl oxygen atom (H**O**OR). The resulting pre-reaction complex then reacts to form RO-Cu^{2+}-OH, where the hydroperoxide O-O bond has been cleaved. Transition states were optimized for the breakdown of one species to liberate free radicals, $HO^{\bullet}$ and $RO^{\bullet}$, regenerating Cu(II). However, this conversion required significant quantities of energy to be put into the system. Moreover, some stationary points on the reaction coordinate were not located and had to be estimated. This study concluded that the O-O cleavage reaction is endoergic. Moreover, the energy required is significantly higher than that needed for thermal fission of peroxides, which is generally around 40-45 kcal mol^{-1}. Therefore, reference 20 concluded that this mechanism is not responsible for the faster degradation of fuels in the presence of copper. This led us to consider whether Cu(I) ions or complexed copper species might react with hydroperoxides more readily than Cu(II).

Herein we look into the decomposition reactions of various peroxides by bare Cu(I) ions and copper naphthenate (Cu(Nap)). We employed density functional theory (DFT) to construct energy profiles and calculate the corresponding thermodynamic data. The implications that the results might have for jet fuel autoxidation and how these results can be integrated into predictive kinetic mechanisms were also considered.

2. Computational Details

All calculations in the main text were performed using Gaussian 09 software, version D.01[29] All calculations employed the use of the B3LYP functional.[26-28] The cc-pVTZ[30] basis set was used for all elements except for copper for which a SDD[31] basis set was used instead. In all calculations the solvent was accounted for using the PCM method as implemented in Gaussian.[32] The solvent parameters for dodecane were used throughout.[33] Geometry optimizations were confirmed as local minima by the absence of imaginary frequencies in the vibrational spectra. Transition states were optimized using the QST3 method as implemented in Gaussian.[34] All transition states were confirmed both *via* the presence of one imaginary frequency corresponding to the saddle point and with intrinsic reaction coordinate (IRC) scans. An ultrafine grid was employed for all calculations with no symmetry constraints. All structures were calculated as singlets with the HOMO and LUMO orbitals mixed (guess=mix option) in order to break the symmetry of the system. Free energies were calculated using the Grimme quasiharmonic entropy correction using the GoodVibes script. [35, 36] Equivalent calculations to those found in the main text employing a larger basis set on the copper atom (cc-pVTZ) and the m06 functional[37] are presented in the supporting information.

3. Results and Discussion

3.1 Reaction of Cumene hydroperoxide and Cu(I)

As mentioned above, thermal decomposition of hydroperoxides requires 40-45 kcal mol^{-1} and is a barrierless process.[18] Any new potential mechanism must therefore provide an alternative pathway that requires less energy. The first step of study was to investigate whether the presence of Cu(I) ions in fuels could facilitate the decomposition of hydroperoxides. Thus, the gibbs energy profile for the reaction of copper and cumene hydroperoxide (CHP) was constructed. A bare Cu(I) ion was initially selected over complexed Cu(I) with a ligand to reduce the computational cost of the calculations. Moreover, this reduced the number of isomers that could be accessed by the presence of a bulky ligand. Cumene hydroperoxide was selected as a model fuel hydroperoxide.

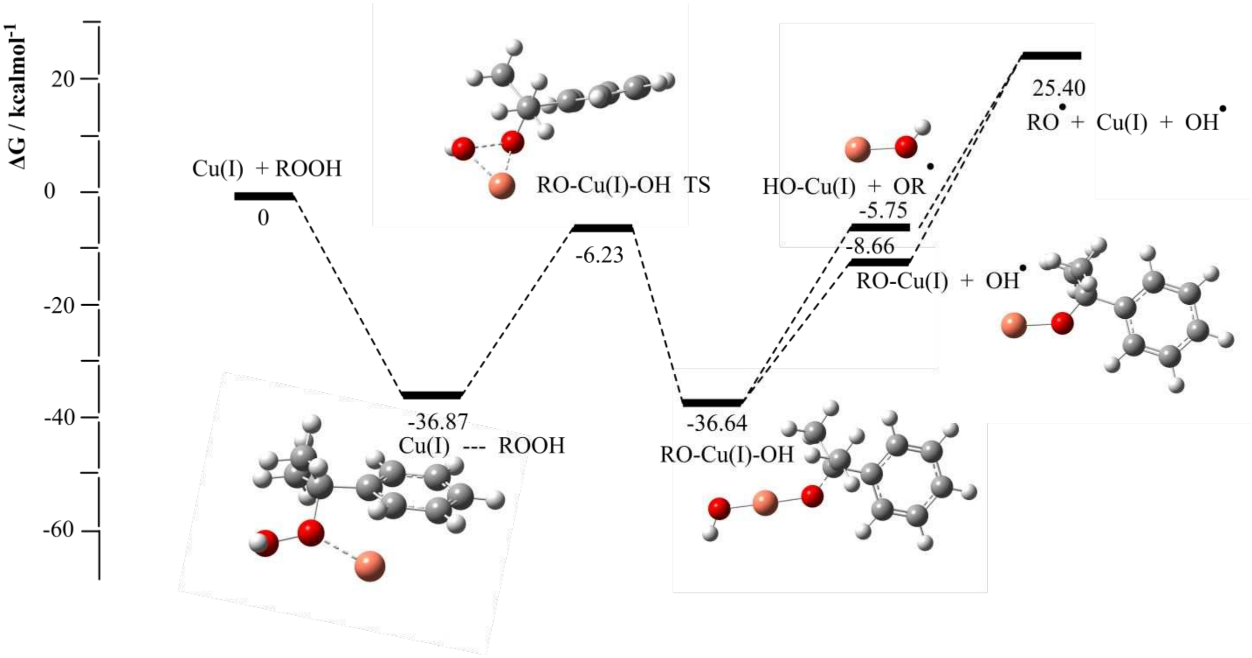

Figure 2. Gibbs free energy profile for the decomposition of CHP *via* Cu(I) (R = $C(CH_3)_2Ph$)

The gibbs energy profile is shown in Figure 2. Four distinct binding interactions were found for the pre-reaction complex, Cu(I)---ROOH, (defined as the structure immediately preceding the transition state where the two reactants are in close proximity). These structures are shown in Figure 3. The copper ion can bind to the peroxide through both oxygen atoms (**1d)**, through either oxygen individually (**1a**, **1b**) or to the phenyl ring (**1c**). The lowest energy structure is **1a** where the copper ion is bound to the alkoxy oxygen of the hydroperoxide (R**<u>O</u>**OH). This isomer is 7.41 kcal mol^{-1} more stable than the next most stable isomer **1c.** The complex is further stabilized by the presence of an η2 interaction with the phenyl ring. As a consequence, more than 99 % of pre-reaction complexes will exist as **1a**, which is 36.87 kcal mol^{-1} more stable than the unbound reactants. As the copper ion is positively charged, and hence electron deficient, the favourable binding to the oxygen atoms is expected as is the strongly exoergic binding energy.

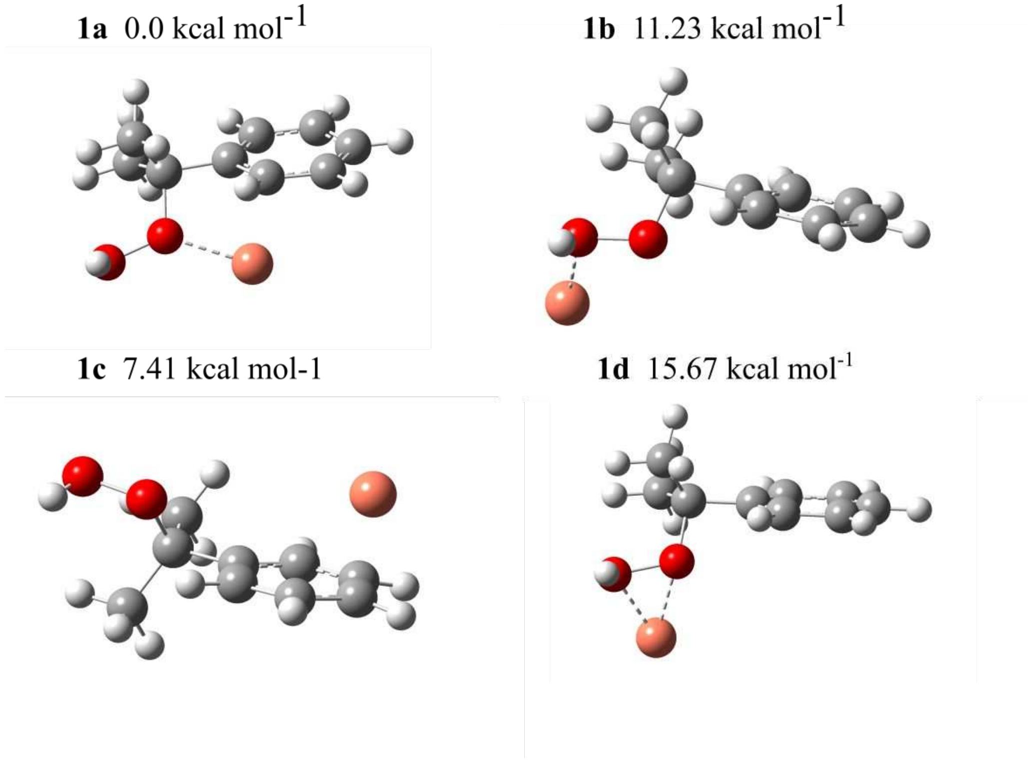

Figure 3. Four possible binding modes of the pre-reaction complex, Cu(I)---ROOH (**1a-1d**). **1a** bound through the alkoxy oxygen (ROOH), **1b** bound through the hydroxy oxygen (ROOH), **1c** bound to the ring. **1d** bound through both oxygen atoms. **1a** is the most stable structure.

From the lowest energy pre-reaction complex the nature of the transition state, RO-Cu(I)-OH TS was investigated. As shown in Figure 4, the copper ion is almost equidistant to both oxygen atoms in this structure (distances of 1.898 and 1.936 Å). The oxygen-oxygen bond has lengthened to 1.93 Å compared to 1.44 Å in the pre-reaction complex. The activation gibbs energy for the reaction is 30.64 kcal mol^{-1}, which is low enough for a reaction to proceed under standard operating conditions. The transition state is still 6.23 kcal mol^{-1} lower in energy than the separated reactants.

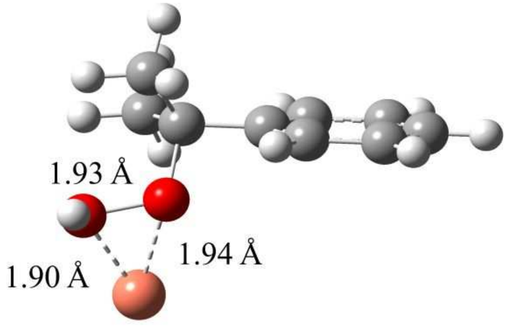

Figure 4. Optimized transition state geometry for RO-Cu(I)-OH TS

In the product complex, RO-Cu(I)-OH, the hydroperoxide O-O bond has been cleaved and both radicals are bound to the copper ion. The complex is approximately linear with an O-Cu-O angle of 174° and is 36.64 kcal mol^{-1} more stable than the separated reactants. This is of similar stability to the most stable pre-reaction complex, **1a**, (36.87 kcal mol^{-1}) which suggests that both will exist in equilibrium.

Next, routes to the release of radicals from the product complex were probed. This involved the optimization of multiple species, HO-Cu(I)$^{\bullet}$ + RO$^{\bullet}$, RO-Cu(I)$^{\bullet}$ + HO$^{\bullet}$ and RO$^{\bullet}$ + HO$^{\bullet}$ + Cu(I). HO-Cu(I)$^{\bullet}$ and RO-Cu(I)$^{\bullet}$ can be formed by release of RO$^{\bullet}$ or HO$^{\bullet}$ from RO-Cu(I)-OH, respectively. The final species is a free ionic copper, which has lost both RO$^{\bullet}$ and HO$^{\bullet}$. Figure 2 shows that the HO$^{\bullet}$ is preferentially released over the RO$^{\bullet}$. The relative energy for HO$^{\bullet}$ release over RO$^{\bullet}$ release is 2.91 kcal mol^{-1} although both processes are endergonic. Release of both radicals from RO-Cu(I)-OH requires 62.04 kcal mol^{-1}. Not only is this highly endergonic, it is also appreciably larger than the reported values for thermal fission of peroxides in absence of metals (40-45 kcal mol^{-1})[18]. Therefore, it does not provide a route to peroxide fission, which is more energetically favourable.[38] In light of this our next consideration was whether any other decomposition routes of RO-Cu(I)-OH were feasible.

3.2 Reaction of RO-Cu(I)-OH with hexane and CHP

The low energy complex, HO-Cu(I)-OR, could potentially react with further equivalents of hydroperoxides in conformity with Fenton reactions. Moreover, it could react directly with the bulk fuel, which is in great excess compared to the concentration of HO-Cu(I)-OR. This is the more likely next step, since the concentration of hydroperoxides is relatively low (ppm range) in fuels. To investigate this, we used hexane in the calculations as a model for jet fuel. We expect that the fission free energies will be largely unaffected by this change. This reduced the computational cost of the calculations when compared to modelling C_{10} to C_{14} hydrocarbon chains, due to the lower number of electrons and fewer degrees of freedom.

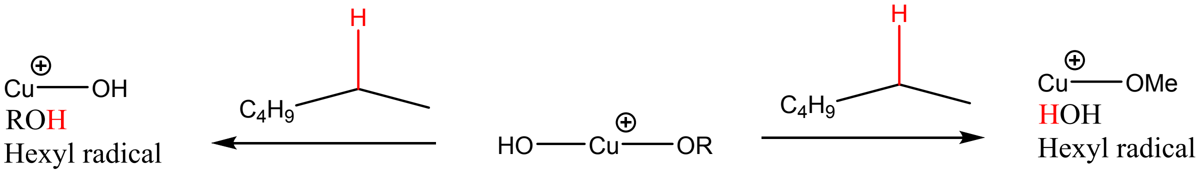

Scheme 1. Two potential decomposition pathways for the reaction of RO-Cu(I)-OH with hexane.

Two routes for the decomposition reaction with hexane were investigated. They are shown in Scheme 1. Thus, either of the bound radicals could abstract a hydrogen from the hexane molecule to yield a hexyl radical and either an alcohol or H_2O dependent on which copper-bound radical reacted.

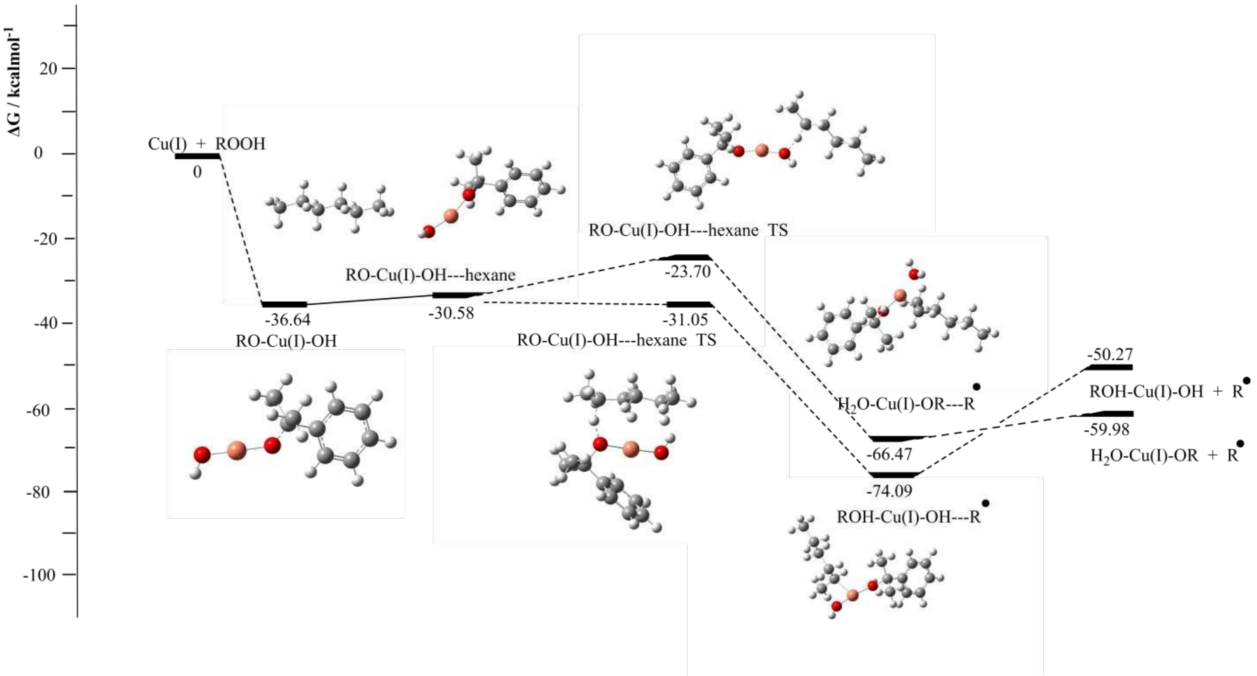

Figure 5. Gibbs free energy profile for the reaction of RO-Cu(I)-OH with hexane.

As can be seen in Figure 5, initial binding of hexane to the copper complex, RO-Cu(I)-OH, carries a free energy cost of 6.29 kcal mol^{-1}. Multiple transition states were located for the proton transfer reactions. These included abstraction of either a terminal hydrogen or a hydrogen from the second carbon in the chain. The most energetically favourable abstraction was from the second carbon in the chain so it is these reactions that are reported here (see Figure 6). The transfer reaction involves a geometry change in the hexane molecule where the geometry around the carbon losing the hydrogen becomes noticeably more planar. The activation free energies are 12.96 and 5.61 kcal mol^{-1} for transfer to OH and OR relative to the separate reactants respectively. The resulting product complexes in both cases contain a hexyl radical. Both products are significantly more stable than the separated reactants, RO-Cu(I)-OH and hexane.

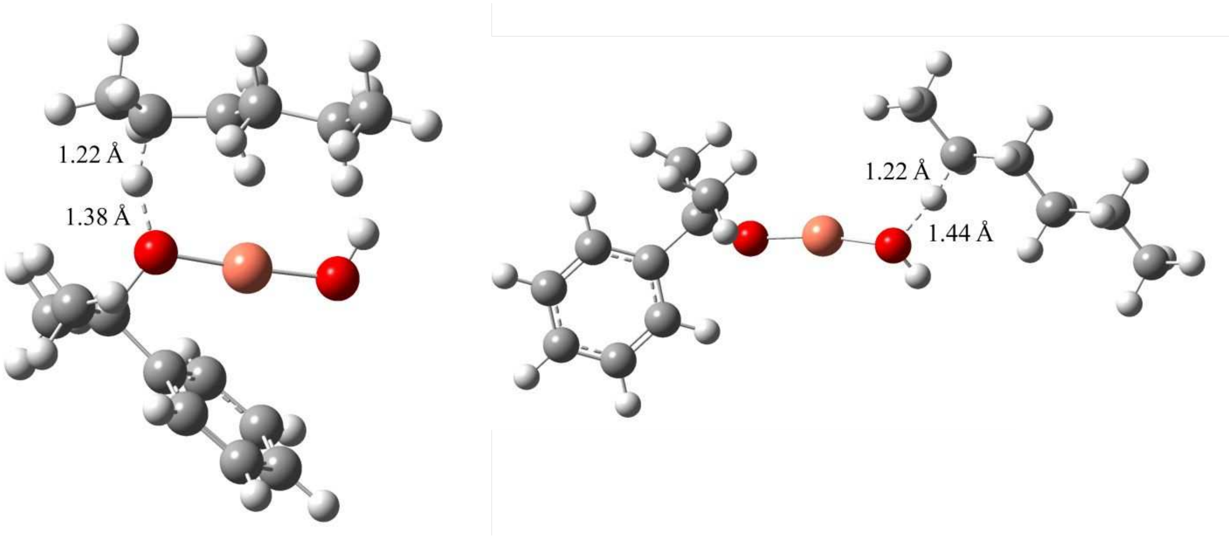

Figure 6. Transition state geometries for the reaction of RO-Cu(I)-OH with hexane. Left: hydrogen transfer to OR. Right: hydrogen transfer to OH.

Removal of the hexyl radical from the product complexes is an endoergic process when viewed in isolation. It is, however, an exoergic process when compared to the reactant species, RO-Cu(I)-OH and hexane. This is of key importance and suggests that copper ions, in the presence of hydroperoxides and paraffins can facilitate the formation of alkyl radical species. These radical species can subsequently play an important role in propagating the autoxidation cycle as mentioned earlier.

Our final consideration was whether RO-Cu(I)-OH could react with further hydroperoxide molecules in a Fenton-like manner as in Scheme 2. Whilst this is not strictly a Fenton mechanism as the charges are different when compared to those in Reaction 5 and Reaction 6, it does bear some similarities. In an analogous manner to the reaction with hexane, the incoming peroxide can react with either of the bound radical molecules in HO-Cu(I)-OR. This reaction results in the formation of a peroxy radical (ROO$^\bullet$) in each case and either water or cumene hydroxide.

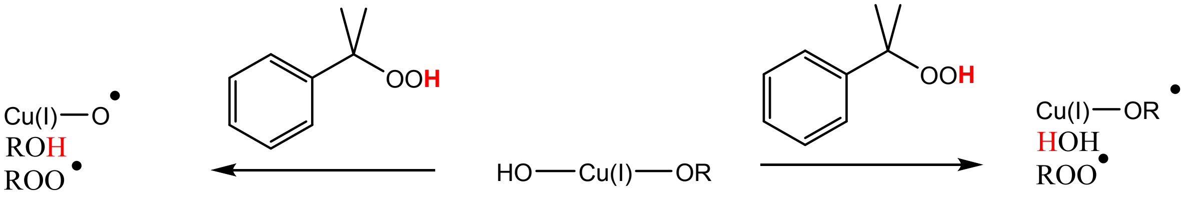

Scheme 2. Two potential decomposition pathways for the reaction of RO-Cu(I)-OH with CHP

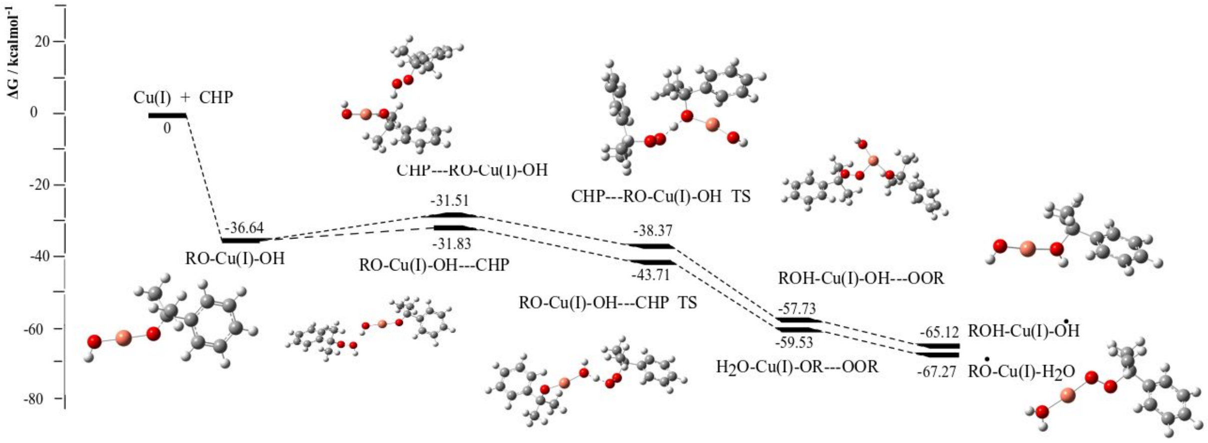

Figure 7. Gibbs free energy profile for the reaction of RO-Cu(I)-OH with CHP.

Two binding interactions were located for the pre-reaction complex, RO-Cu(I)-OH---CHP. The CHP molecule can bind to either end of RO-Cu(I)-OH forming a hydrogen bond in both cases. It was observed that both transition states are lower in energy than the pre-reaction complexes. This is attributed to the formation of neutral, electron-rich species (water and cumene hydroxide), which can stabilize the electron deficient copper ion. Furthermore, the results indicate that the peroxy radical species (ROO$^{\bullet}$), formed by H loss from CHP, is more stable than either of the hydroxy or alkoxy radicals. Also, both product complexes are significantly more stable than the separated reactants, RO-Cu(I)-OH and CHP and removal of the peroxy radical from the product is exoergic. This suggests that RO-Cu-OH can react with hydroperoxides to form stable complexes and peroxy-radicals. However, given that the concentration of peroxides in jet fuel is relatively low, it is likely that the reaction with paraffins is the dominant reaction.

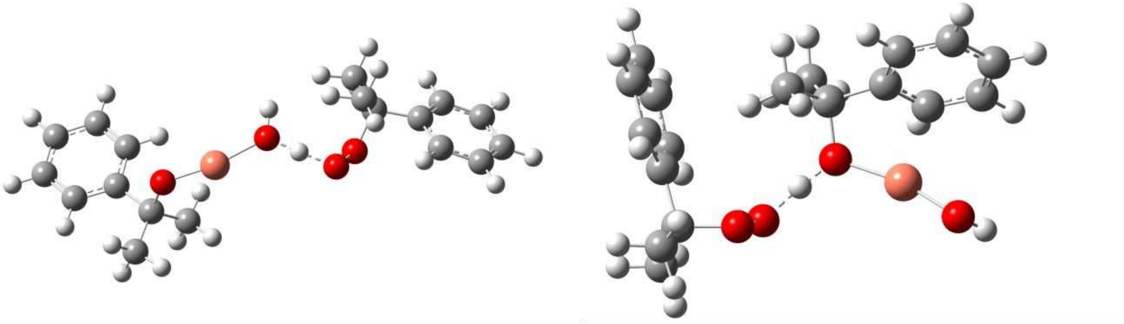

Figure 8. Transition state geometries for the reaction of RO-Cu(I)-OH with CHP. Left: hydrogen transfer to OH. Right: hydrogen transfer to OR.

Thus far, we have shown that Cu(I) ions can react with hydroperoxides to form species containing two bound radicals. This can subsequently go on to react with either hydroperoxides or with paraffins to form radical species which are important in the autoxidation cycle. As has been discussed earlier, the presence of naphthenic acids alongside copper has been shown to accelerate peroxide decomposition. The nature of this acceleration was investigated next.

3.3 Reaction of CHP and Cu(Naphthenate)

Naphthenic acids are naturally found in crude oil and consequently are present in jet fuels. They could potentially react with copper to form fuel soluble metal salts. Not only will this aid the dissolution of the copper in fuel, it could have a profound effect on the reaction with hydroperoxides by changing both the electronic nature of, and steric environment around, the metal. The reaction as shown in Scheme 3 was therefore investigated in an analogous manner to that for Cu(I).

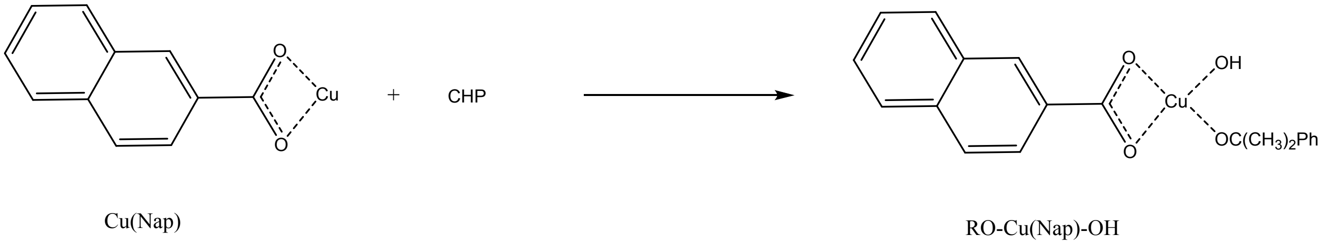

Scheme 3. Proposed reaction scheme for the copper-mediated decomposition of CHP.

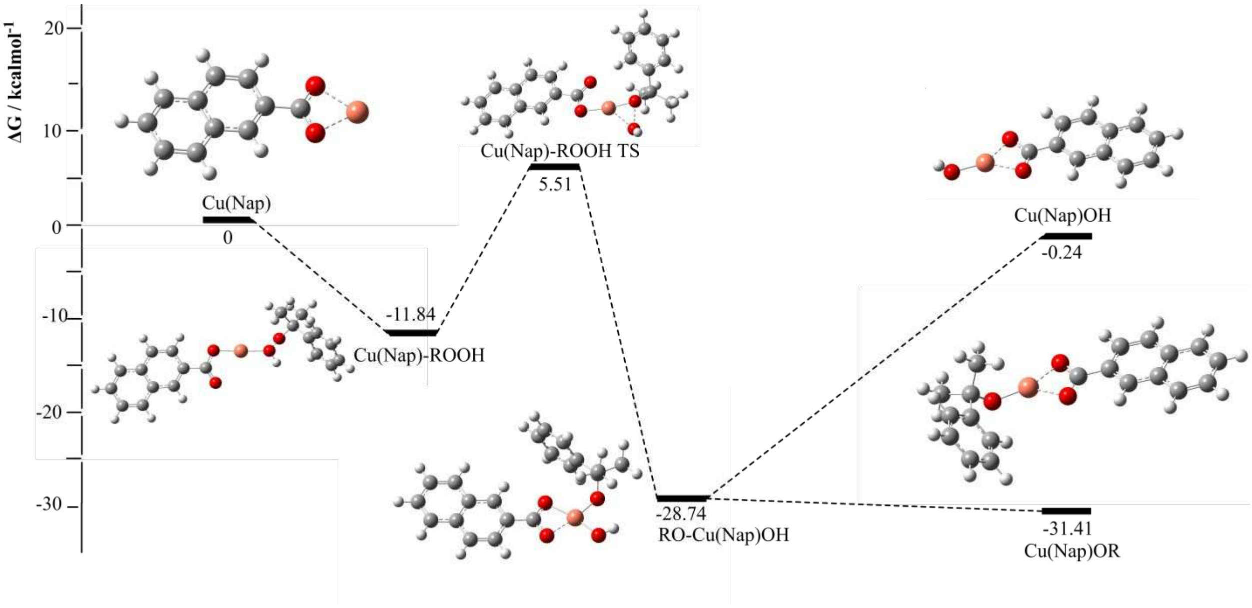

Figure 9. Gibbs free energy profile for the decomposition of CHP by Cu(Nap).

The DFT-calculated reaction profile is shown in Figure 9. The copper ion in the reactant molecule, Cu(Nap), is equidistant to both oxygen atoms (distances of 2.08 Å). Interestingly, in the pre-reaction complex, Cu(Nap)-ROOH, the naphthenate anion is bound to the copper ion through one oxygen atom only (Cu-O distances of 1.85 Å to the bound oxygen and 2.78 Å to the unbound oxygen) as can be seen in Figure 10. Multiple different starting geometries were investigated for this complex, which all converged to the same structure. The hydroperoxide is bound to the copper atom through the hydroxyl (-<u>O</u>H) oxygen atom. This is in contrast to the geometries observed for Cu(I)---ROOH where four distinct geometries were found. This binding interaction of the hydroperoxide and copper naphthenate represents an energy gain of 11.84 kcal mol^{-1} compared to the separated reactants. A similar motif is observed in the transition state (Cu(Nap)-ROOH TS) where the naphthenate anion binds to the copper atom as a monodentate ligand. The activation free energy for this reaction is 16.94 kcal mol^{-1}, which is lower than that observed for bare copper ions (30.64 kcal mol^{-1}). This supports the observation that copper is more reactive towards peroxides in the presence of naphthenates. The product complex, RO-Cu(Nap)OH, adopts a square planar structure where the naphthenate anion is bound to the copper through both oxygen atoms (distances of 1.95 Å). The products are 28.74 kcal mol^{-1} more stable than the separated reactants indicating there is a significant driving force for the reaction.

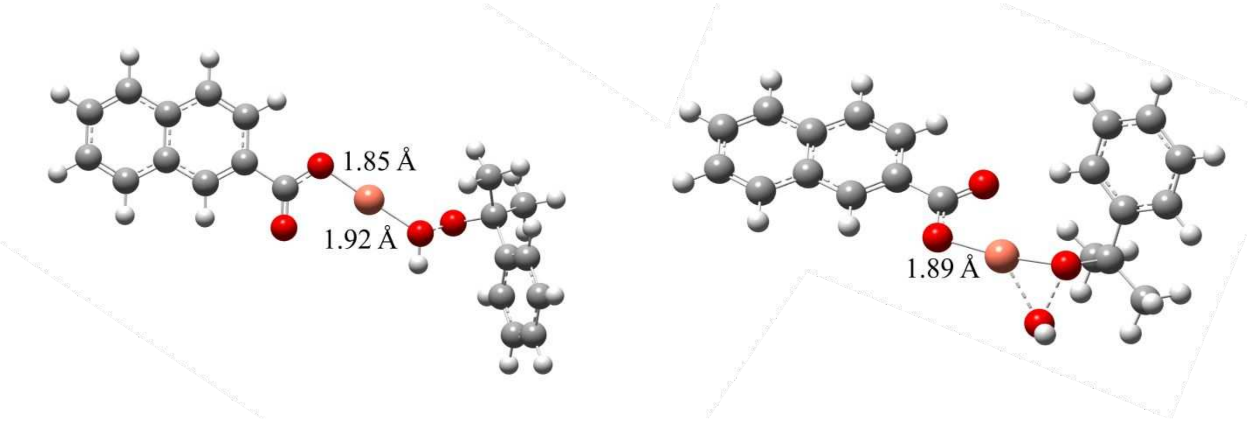

Figure 10. Optimized geometries for the pre-reaction complex Cu(Nap)-ROOH (Left) and the transition state for reaction with CHP (Right)

Comparison of Figure 2 with Figure 9 shows that in contrast to the reaction of free copper ions with CHP, the product of the decomposition of CHP with copper naphthenate is both thermodynamically and kinetically favoured. For bare Cu(I), the reactant and product complexes are in equilibrium. The liberation of free radicals in particular from RO-Cu(Nap)OH is not as unfavourable as it is for liberation from the bare copper ion. Indeed, removal of the alkoxy radical ($RO^{\bullet}$) from RO-Cu(Nap)OH to form HO-Cu(Nap) is favoured by 2.67 kcal mol^{-1}. Despite the liberation of radicals from the product complex being favoured, it was still of interest to investigate the reaction of RO-Cu(Nap)OH with hexane for comparison with the bare copper system.

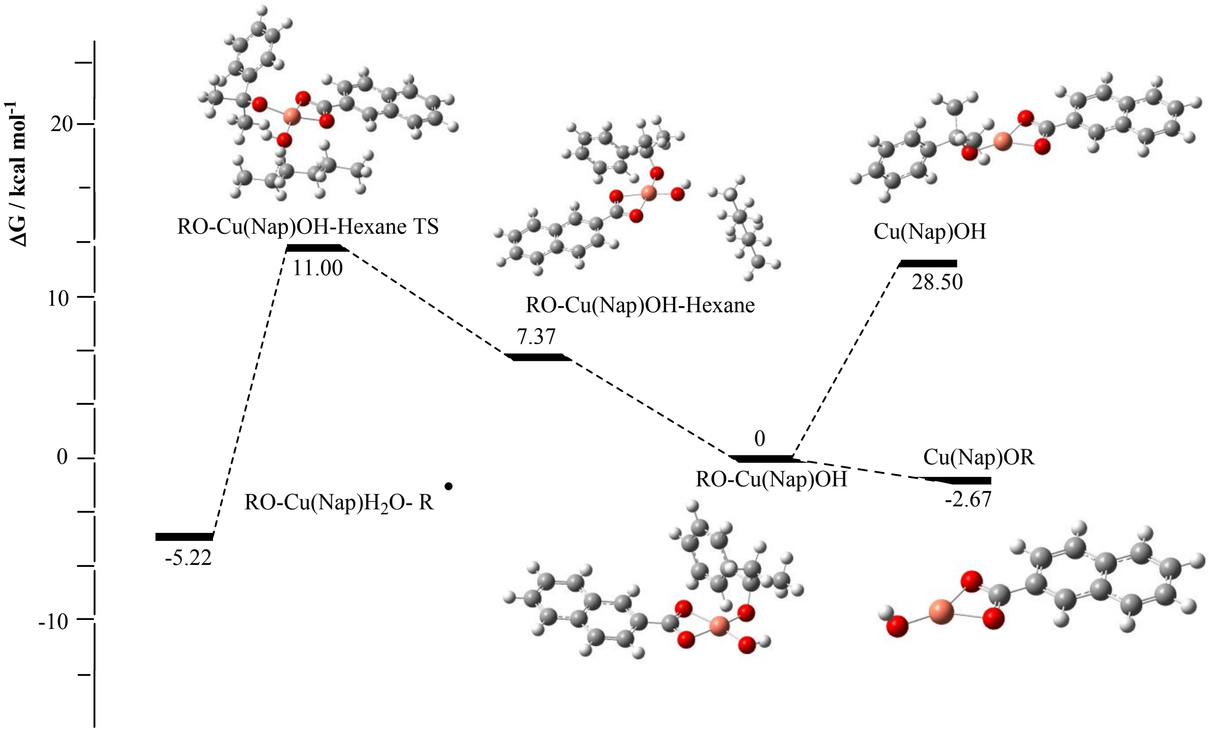

Figure 11. Gibbs free energy profile for the decomposition reaction of RO-Cu(Nap)OH and hexane

Initially, an equivalent reaction was investigated as to that postulated in Scheme 1, where a hexane molecule reacts with either the alkoxy ($RO^{\bullet}$) or hydroxyl ($HO^{\bullet}$) radical bound to the copper centre. Initial binding of hexane to the copper complex RO-Cu(Nap)OH carries a free energy cost of 7.37 kcal mol^{-1} as a consequence of fixing the orientation of both molecules. Despite repeated attempts, the transition state for the transfer to the bound alkoxy radical could not be located. This was attributed to the steric bulk of both the naphthenate anion and the radical itself hindering the approach of the hexane molecule. However, the transition state for the transfer to OH was located. In this transition state, the hydroxyl radical is moving away from the copper centre. At the same time, a hydrogen is approaching from the hexane molecule to form a water molecule. The activation free energy for the reaction is 11 kcal mol^{-1}, which is greater than that observed for the equivalent reaction with the bare copper. The reaction is thermodynamically favoured with the products been 5.22 kcal mol^{-1} more stable than the separated reactants. Despite this reaction having a low activation energy, it is still higher than liberation of a radical from RO-Cu(Nap)OH, which is therefore likely to be the dominant reaction when both copper and naphthenates are present.

3.4 Further reactions of hydroperoxides and Cu(Nap)

A potential mechanism that can produce radicals from hydroperoxides and copper, both bare and in the presence of naphthenates, has been postulated. It was of interest, therefore, to expand the work to investigate a wider range of hydroperoxide species. Undoubtedly there could be a multitude of different peroxides present in fuels formed from the paraffinic fuel or from aromatic compounds. Hence, the effect of changing the hydroperoxide on the reaction with copper naphthenate was modelled. The peroxides selected for this investigation are illustrated in Figure 12.

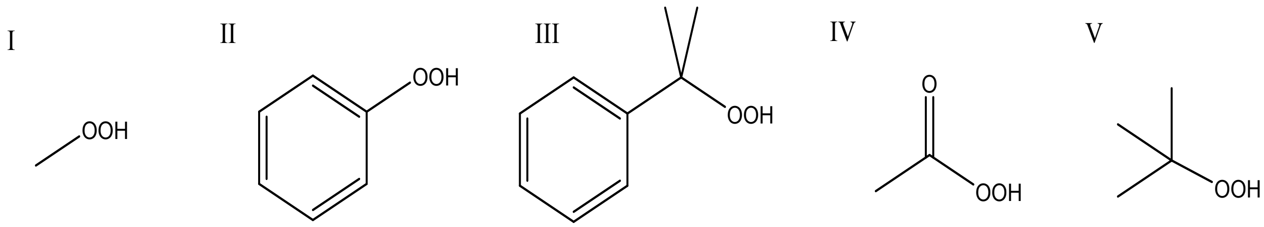

Figure 12. Further peroxide molecules investigated, methyl peroxide (I), phenyl hydroperoxide (II), cumene hydroperoxide (III), peracid (IV) and *tert*-butylhydroperoxide (V)

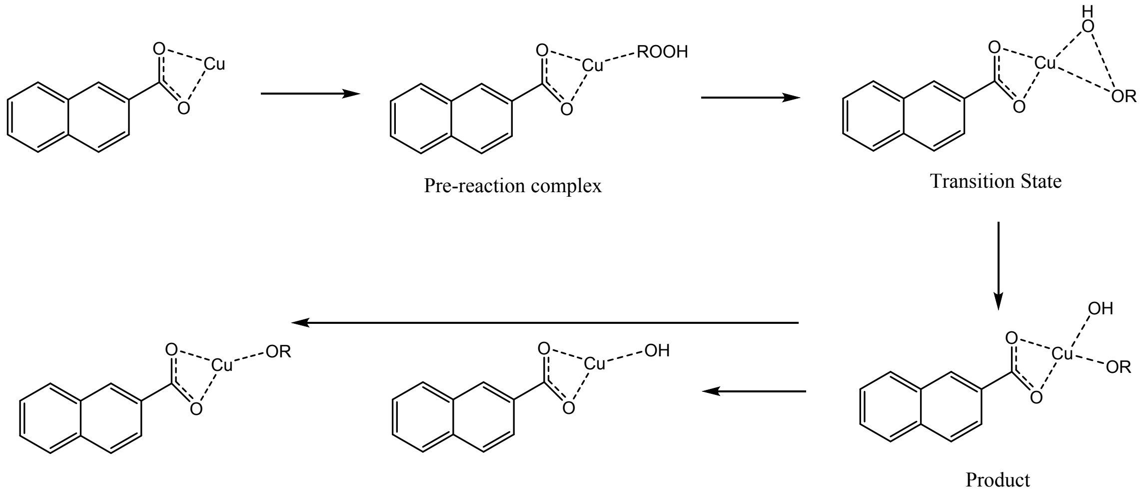

Scheme 4. General scheme showing the complexes required to construct an energy profile for the metal-catalyzed decomposition of peroxides. (R = Me, Ph, CH_3CO, ^tBu, $C_6H_5C(CH_3)_2$)

Scheme 4 shows the complexes required to calculate the thermochemical parameters for the decomposition of each hydroperoxide. The corresponding thermodynamic data is given in Table 1. The energetics of the initial binding of the peroxide to the metal complex in the pre-reaction complex are similar for each of the peroxides investigated. In each case, the interaction is exoergic. The activation gibbs energies range from 11.06 kcal mol^{-1} for PhOOH to 16.94 kcal mol^{-1} for cumene hydroperoxide. The most stable product results from the reaction with PhOOH. This is likely due to the increased stabilization that the radical species experiences in the product. In $^{\bullet}$OPh, the radical is stabilized *via* resonance delocalization through the ring. This data implies that aromatic peroxides would be more important for the autoxidation cycle compared to alkyl peroxides and facilitate faster production of radicals.

Table 1. DFT-calculated thermodynamic data for peroxide decomposition with Cu(Nap)

Peroxide	ΔG / kcal mol^{-1}			
	Pre-reaction	**Transition State**	**Product**	**E_a**
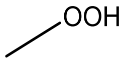	-10.58	5.67	-28.74	16.25
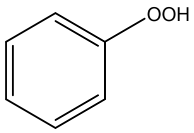	-10.95	0.11	-38.78	11.06
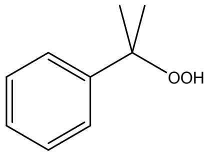	-11.84	5.10	-28.74	16.94
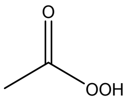	-5.67	9.91	-35.16	15.58
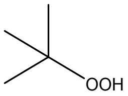	-10.35	5.81	-29.11	16.16

3.5 Mechanistic implications

The work undertaken herein has shown that metals have an important role in mediating the decomposition of hydroperoxides and furthermore can potentially undergo decomposition reactions to form alkyl radicals and/or peroxy radicals. Hence the chemistry of metals is of key importance in producing a more robust kinetic model for autoxidation, particularly the initiation step which is hitherto poorly understood. Currently, the only reaction in the Kuprowicz mechanism that takes metals into consideration is Reaction 7, shown in table 2. In order to more accurately represent the reactions that potentially could occur, we would propose supplementing Reaction 7 with Reactions 8 - 12.

Table 2. Proposed steps to improve current chemical kinetic mechanisms.

Reaction	Source	Label
$ROOH + \text{“M”} \longrightarrow RO^{\bullet} + HO^{\bullet}$	Ref 12.	(7)
$ROOH + CuL \longrightarrow RO^{\bullet}\text{-}CuL\text{-}HO^{\bullet}$	This work	(8)

$$RO^{\bullet}\text{-}CuL\text{-}HO^{\bullet} \longrightarrow RO^{\bullet}\text{-}CuL + HO^{\bullet} \qquad \text{This work} \qquad (9)$$

$$RO^{\bullet}\text{-}CuL\text{-}HO^{\bullet} \longrightarrow HO^{\bullet}\text{-}CuL + RO^{\bullet} \qquad \text{This work} \qquad (10)$$

$$RO^{\bullet}\text{-}CuL\text{-}HO^{\bullet} + R'H \longrightarrow RO^{\bullet}\text{-}CuL + R^{\bullet\prime} + H_2O \qquad \text{This work} \qquad (11)$$

$$RO^{\bullet}\text{-}CuL\text{-}HO^{\bullet} + R'OOH \longrightarrow RO^{\bullet}\text{-}CuL + ROO^{\bullet\prime} + H_2O \qquad \text{This work} \qquad (12)$$

These reactions describe the decomposition of the hydroperoxide species (Reaction 8), the liberation of hydroxy and alkoxy radicals, (Reactions 9-10), the production of alkyl radicals (Reaction 11) and the reaction with hydroperoxides (Reaction 12). Once appropriately validated, these additions should help to improve the predictive capabilities of the kinetic mechanism. This will be the subject of a further publication.

4. Conclusions

The understanding of how trace metal impurities detrimentally affect the lifetime of jet fuel is of critical importance to improving the lifetime of future fuels. In this work we have reported on the DFT calculations on the reactions of various copper complexes with common hydroperoxides found in jet fuels. The reaction of the product complexes with paraffins and peroxides were also investigated.

The reaction of CHP with Cu(I) ions was found to produce a mixture of species. The pre-reaction complex, Cu(I)---ROOH, and the product complex, RO-Cu(I)-OH, exist in approximately a 1:1 ratio. The product complex, RO-Cu(I)-OH does not favourably liberate either of the bound radicals, $RO^{\bullet}$ and $HO^{\bullet}$. The energy required is greater than for thermal breakdown of free peroxides. However, subsequent reactions of RO-Cu(I)-OH with either paraffins or peroxides can produce alkyl radicals and peroxy radicals respectively. Both of these reactions are favoured thermodynamically and provide an alternative route to radical formation in fuels given the presence of copper, peroxides and paraffins provided that the reaction is rapid.

In contrast to the reaction of hydroperoxides with bare copper ions, the reaction of Cu(Nap) with CHP to form RO-Cu(Nap)OH is thermodynamically favoured forming only one product complex. The reaction of this species with either paraffins or peroxides is not as favoured as for free copper. Furthermore, both of these reactions have higher activation energies than for liberation of free radicals, $RO^{\bullet}$ and $HO^{\bullet}$, from RO-Cu(Nap)OH.

It can be concluded therefore that copper ions in the presence of naphthenic acids can form fuel soluble metal complexes. These can go onto react with peroxides to produce radicals more easily than can be produced by thermal decomposition of peroxides in absence of copper.

The current literature mechanisms for predicting the autoxidative behavior of jet fuels can likely be further improved by replacing the existing single reaction involving metals with a more detailed series of reactions we have presented herein.

Supporting Information

Cartesian coordinates for DFT-optimized structures.

Equivalent calculations to those in the main text, except using the m06 functional and employing cc-pVTZ basis set on the copper.

Author information

ORCID

Ehsan Alborzi: 0000-0002-2585-0824

Anthony J. H. M. Meijer: 0000-0003-4803-3488

Christopher Parks: 0000-0001-8016-474X

The authors declare no competing financial interest.

Acknowledgments

The work described in this paper was funded by the EU Clean Sky 2 programme FINCAP ("Fuel INjector Coking and Autoxidation Prediction), grant number 755606

References

1. Hazlett, R. N., Thermal Oxidation Stability of AViation Turbine Fuels; . *ASTM: Philadelphia* **1991**.

2. Taylor, W. F., Deposit Formation from Deoxygenated Hydrocarbons. II. Effect of Trace Sulfur Compounds *Ind. Eng. Chem. Prod. Res. Dev.* **1976,** *15*, 64−68.

3. Zabarnick, S.; Mick, M. S., Inhibition of Jet Fuel Oxidation by Addition of Hydroperoxide-Decomposing Species. *Ind. Eng. Chem. Res.* **1999,** *38*, 3557−3563.

4. Balster, L. M.; Zabarnick, S.; Striebich, R. C.; Shafer, L. M.; West, Z. J., Analysis of Polar Species in Jet Fuel and Determination of Their Role in Autoxidative Deposit Formation. *Energy Fuels* **2006,** *20*, 2564−2571.

5. Commodo, M.; Fabris, I.; Groth, C. P. T.; Gülder, O. L., Analysis of Aviation Fuel Thermal Oxidative Stability by Electrospray Ionization Mass Spectrometry (ESI−MS). *Energy Fuels* **2011,** *25*, 2142−2150.

6. Ervin, J. S.; Williams, T. F., Dissolved Oxygen Concentration and Jet Fuel Deposition. *Ind. Eng. Chem. Res.* **1996,** *35*, 899−904.

7. Striebich, R. C.; Contreras, J.; Balster, L. M.; West, Z.; Shafer, L. M.; Zabarnick, S., Identification of Polar Species in Aviation Fuels using Multidimensional Gas Chromatography-Time of Flight Mass Spectrometry. *Energy Fuels* **2009,** *23*, 5474−5482.

8. Taylor, W. F.; Frankenfeld, J. W., Deposit Formation from Deoxygenated Hydrocarbons. 3. Effects of Trace Nitrogen and Oxygen Compounds. *Ind. Eng. Chem. Prod. Res. Dev.* **1978,** *17*, 86−90.

9. Grinstead, B.; Zabarnick, S., Studies of Jet Fuel Thermal Stability, Oxidation, and Additives Using an Isothermal Oxidation Apparatus Equipped with an Oxygen Sensor. *Energy Fuels* **1999,** *13*, 756−760.

10. Jones, E. G.; Balster, L. M., Impact of Additives on the Autoxidation of a Thermally Stable Aviation Fuel. *Energy Fuels* **1997,** *11*, 610-614.

11. Hazlett, R. N., Thermal Oxidation Stability of Aviation Turbine Fuels;. *ASTM* **1991**.

12. Kuprowicz, N. J.; Zabarnick, S.; West, Z. J.; Ervin, J. S.; Edwards, T., Use of Measured Species Class Concentrations With Chemical Kinetic Modelling for the Prediction of Autoxidation and Deposition of Jet Fuels. *Energy Fuels* **2007,** *21*, 530−544.

13. Pickard, J. M.; Jones, E. G., Catalysis of Jet-A Fuel Autoxidation by Fe2O3. *Energy Fuels* **1997,** *11*, 1232−1236.

14. Jones, E. G.; Balster, W. J., Phenomenological Study of the Formation of Insolubles in a Jet-A Fuel. *Energy Fuels* **1993,** *7*, 968− 977.

15. Jones, E. G.; Balster, L. M.; Balster, W. J., Autoxidation of Aviation Fuels in Heated Tubes : Surface Effects. *Energy Fuels* **1996,** *10*, 831−836.

16. Kuprowicz, N. J.; Ervin, J. S.; Zabarnick, S., Modeling the liquidphase oxidation of hydrocarbons over a range of temperatures and dissolved oxygen concentrations with pseudo-detailed chemical kinetics. *Fuel* **2004,** *83*, 1795−1801.

17. Denisov, E. T.; Afanas'ev, I. B., Oxidation and Antioxidants in Organic Chemistry and Biology. *CRC Press* **2005**.

18. Sebbar, N.; Bockhorn, H.; Bozzelli, J. W., *Phys. Chem. Chem. Phys.* **2002,** *4*, 3691-3703.

19. Mushrush, G. W.; Beal, J. E.; Slone, E.; Hardy, D. R., *Energy Fuels* **1996,** *10*, 504-508.

20. G., S., Atmospheric Oxidation and Antioxidants. *Elsevier, New York* **1965**.

21. Reich, L.; Stivala, S. S., Autoxidation of Hydrocarbon and Polyolefins Kinetics and Mechanisms. **1969**.

22. Winterbourn, C. C., Toxicity of iron and hydrogen peroxide: the Fenton reaction *Toxicology Letters 82/83* **1995** 969-974

23. Bridgeman, C., *SAE J* **1932,** *30*, 207.

24. Peterson, C. J., *Ind. Eng. Chem.* **1949,** *41*, 924-928.

25. Zabarnick. S; K., P. D., Density Functional Theory Calculations of the Energetics and Kinetics of Jet Fuel Autoxidation Reactions. *Energy & Fuels* **2006,** (20), 488-497.

26. Becke, A. D., Density-functional exchange-energy approximation with correct asymptotic behavior. *Phys. Rev. A.* **1988,** (38), 3098.

27. Lee, C.; Yang, W.; Parr, R. G., Development of the Colle-Salvetti correlation-energy formula into a functional of the electron density. *Phys. Rev. B.* **1988,** (32), 785.

28. Perdew, P.; Chevary, J. A.; Vosko, S. H.; Jackson, K. A.; Pederson, M. R.; Singh, D. J.; Fiolhais, C., Atoms, molecules, solids, and surfaces: Applications of the generalized gradient approximation for exchange and correlation. *phys. Rev. B.* **1992,** (46), 6671.

29. Gaussian 09, R. D., M. J. Frisch, G. W. Trucks, H. B. Schlegel, M. A. Robb, J. R. Cheeseman, G. Scalmani, V. Barone, G. A. Petersson, H. Nakatsuji, X. Li, M. Caricato, A. Marenich, J. Bloino, B. G. Janesko, R. Gomperts, B. Mennucci, H. P. Hratchian, J. V. Ortiz, A. F. Izmaylov, J. L. Sonnenberg, D. Williams-Young, F. Ding, F. Lipparini, F. Egidi, J. Goings, B. Peng, A. Petrone, T. Henderson, D. Ranasinghe, V. G. Zakrzewski, J. Gao, N. Rega, G. Zheng, W. Liang, M. Hada, M. Ehara, K. Toyota, R. Fukuda, J.

Hasegawa, M. Ishida, T. Nakajima, Y. Honda, O. Kitao, H. Nakai, T. Vreven, K. Throssell, J. A. Montgomery, Jr., J. E. Peralta, F. Ogliaro, M. Bearpark, J. J. Heyd, E. Brothers, K. N. Kudin, V. N. Staroverov, T. Keith, R. Kobayashi, J. Normand, K. Raghavachari, A. Rendell, J. C. Burant, S. S. Iyengar, J. Tomasi, M. Cossi, J. M. Millam, M. Klene, C. Adamo, R. Cammi, J. W. Ochterski, R. L. Martin, K. Morokuma, O. Farkas, J. B. Foresman, D. J. Fox, Gaussian, Inc., Wallingford, CT, 2016. .

30. Dunning Jr., T. H., Gaussian basis sets for use in correlated molecular calculations. I. The atoms boron through neon and hydrogen *J. Chem. Phys.* **1989,** (90), 1007.

31. Dolg, M., Relativistic electronic structure theory. *Theor. Comput. Chem.* **2002,** *11*, 793.

32. Frisch, G. S. a. M. J., Continuous surface charge polarizable continuum models of solvation. I. General formalism. *J. Chem. Phys.* **2010,** *132*.

33. Cossi, M.; Barone, V.; Mennucci, B.; Tomasi, Analytical second derivatives of the free energy in solution by polarizable continuum models *J. Chem. Phys. Lett.* **1998,** (286), 253.

34. Cances, M. T.; Mennuci, B.; Tomasi, J., A new integral equation formalism for the polarizable continuum model: Theoretical background and applications to isotropic and anisotropic dielectrics. *J. Chem. Phys.* **1997,** *107*, 3032.

35. Grimme, S., Supramolecular Binding Thermodynamics by Dispersion-Corrected Density Functional Theory. *Chem. Eur. J.* **2012,** *18*, 9955-9964.

36. I. Funes-Ardoiz; Paton, R. S., GoodVibes: Version 2.0.3. *Zenodo* **2018**.

37. Zhao, Y.; Truhlar, D. G., The M06 suite of density functionals for main group thermochemistry, thermochemical kinetics, noncovalent interactions, excited states, and transition elements: two new functionals and systematic testing of four M06-class functionals and 12 other functionals. *Theoretical Chemistry Accounts* **2008,** *120* (1), 215-241.

38. Kozuch, S.; J.M.L., M., The rate-determining step is dead. Long live the rate-determining state! . *ChemPhysChem* **2011,** *12(8)*.

For Table of Contents Only

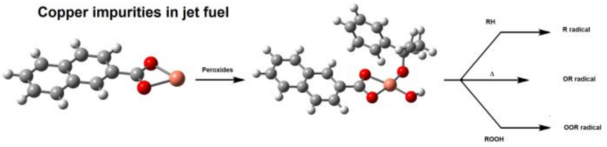
Copper impurities in jet fuel
Peroxides
RH
R radical
Δ
OR radical
ROOH
OOR radical

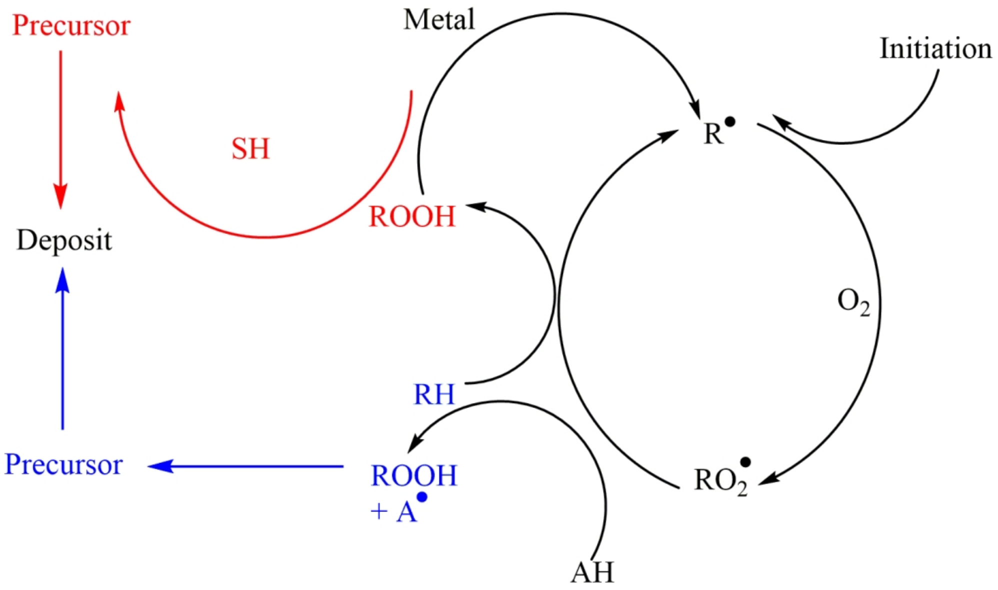

Figure 1. A simplified autoxidation scheme of liquid hydrocarbons highlighting potential routes to deposit formation via sulphurs (SH) and peroxides (ROOH) 12

136x82mm (300 x 300 DPI)

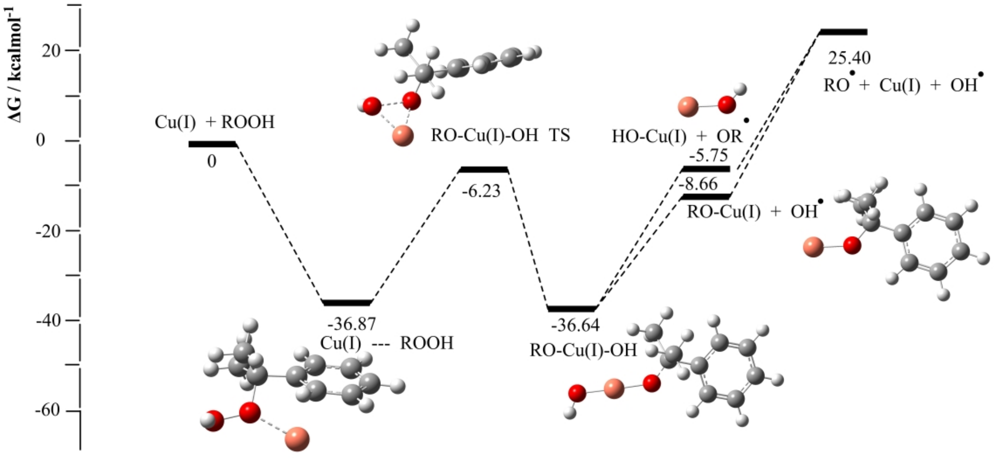

Figure 2. Gibbs free energy profile for the decomposition of CHP via Cu(I) (R = C(CH3)2Ph)

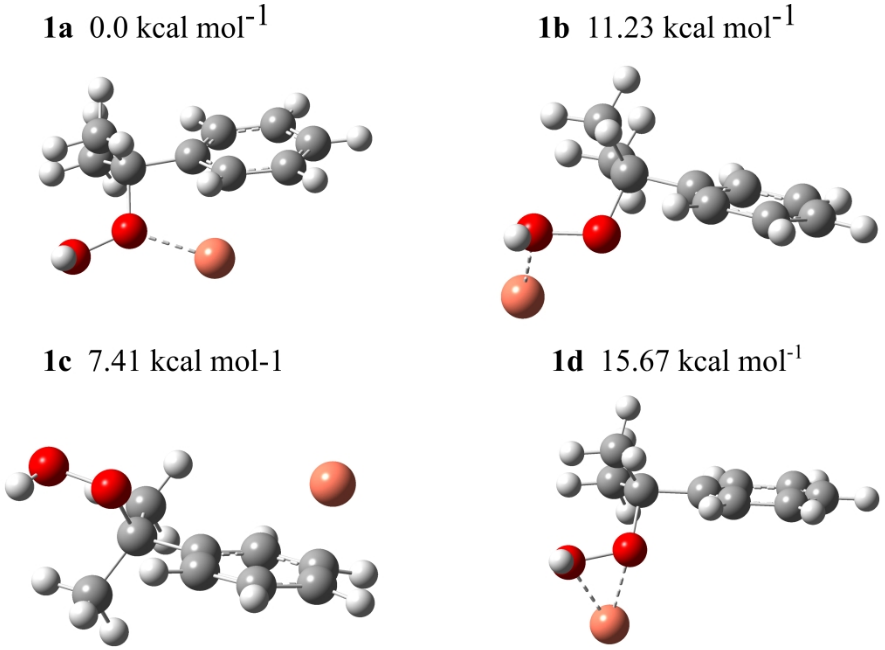

1a 0.0 kcal mol^{-1}

1b 11.23 kcal mol^{-1}

1c 7.41 kcal mol-1

1d 15.67 kcal mol^{-1}

Four possible binding modes of the pre-reaction complex, Cu(I)---ROOH (1a-1d). 1a bound through the alkoxy oxygen (ROOH), 1b bound through the hydroxy oxygen (ROOH), 1c bound to the ring. 1d bound through both oxygen atoms. 1a is the most stable structure.

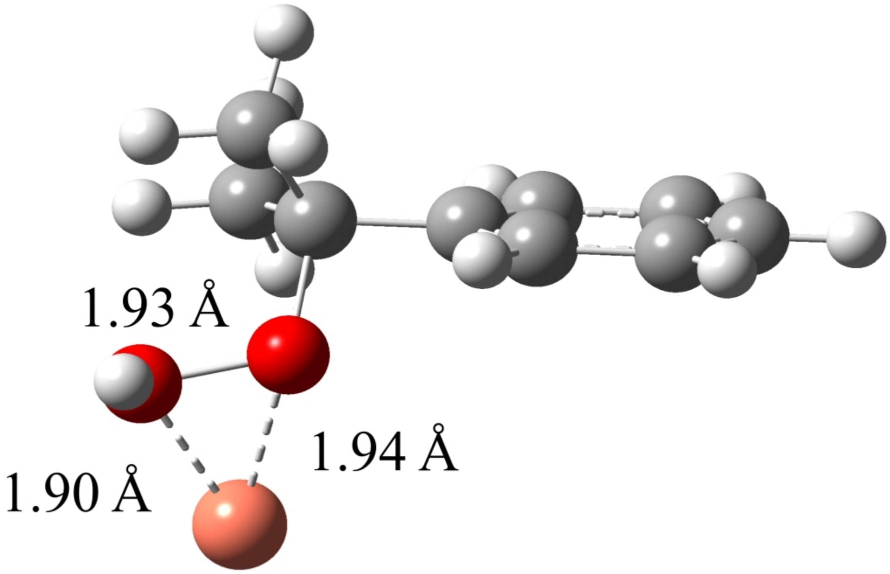

Figure 4. Optimized transition state geometry for RO-Cu(I)-OH TS

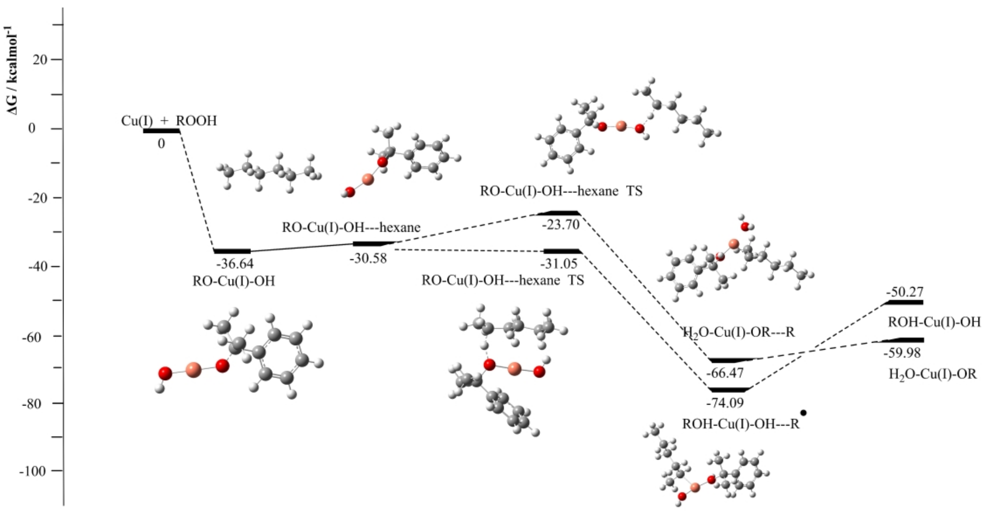

Figure 5. Gibbs free energy profile for the reaction of RO-Cu(I)-OH with hexane.

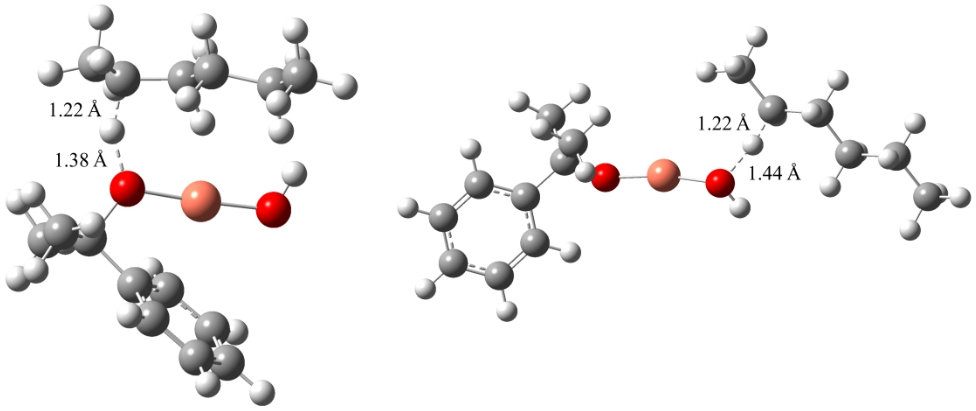

Figure 6. Transition state geometries for the reaction of RO-Cu(I)-OH with hexane. Left: hydrogen transfer to OR. Right: hydrogen transfer to OH.

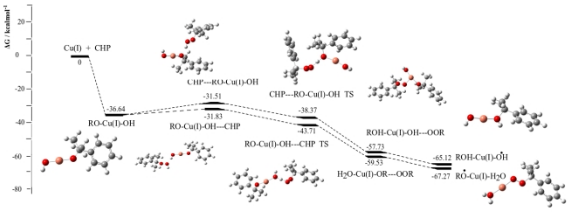

Caption : Figure 7. Gibbs free energy profile for the reaction of RO-Cu(I)-OH with CHP.

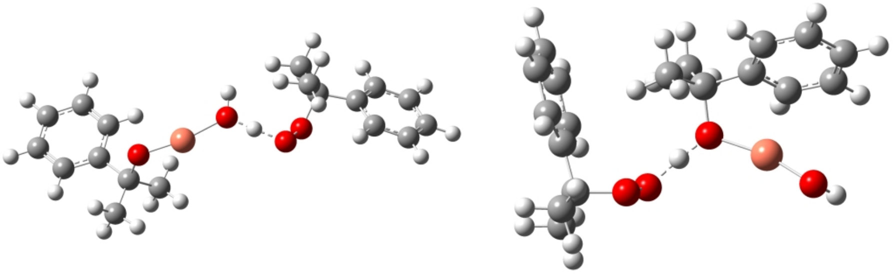

Transition state geometries for the reaction of RO-Cu(I)-OH with CHP. Left: hydrogen transfer to OH. Right: hydrogen transfer to OR

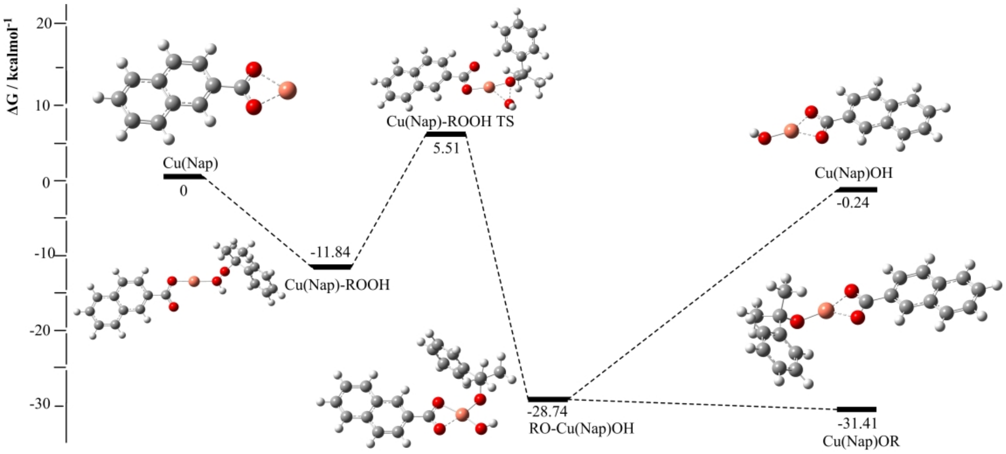

Figure 9. Gibbs free energy profile for the decomposition of CHP by Cu(Nap).

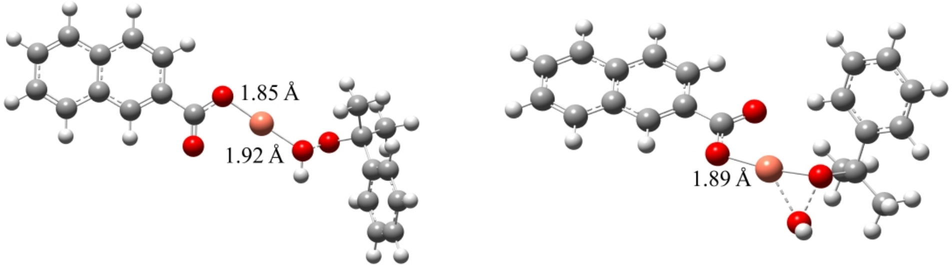

Figure 10. Optimised geometries for the pre-reaction complex Cu(Nap)-ROOH (Left) and the transition state for reaction with CHP (Right)

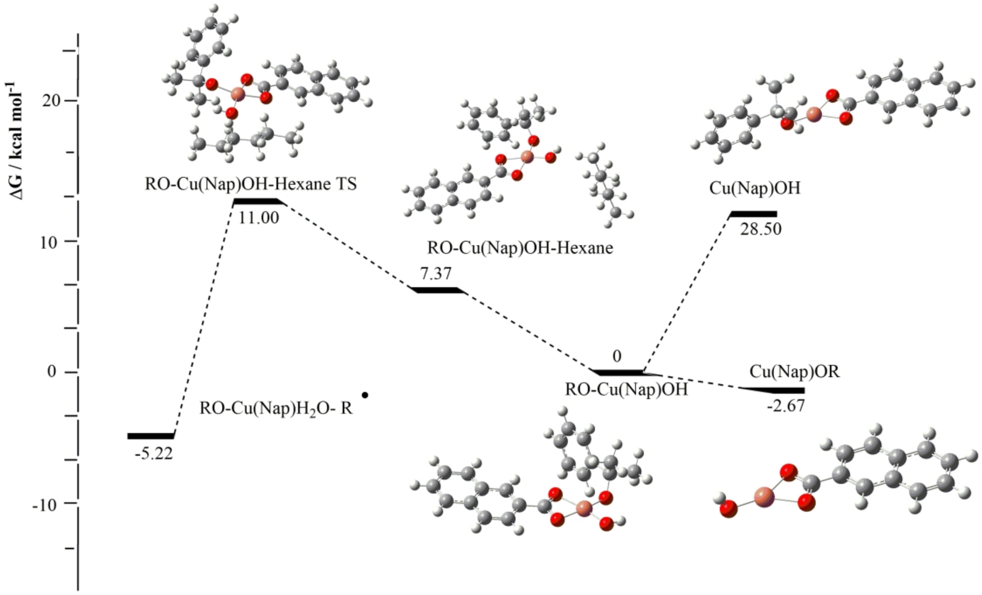

Figure 11. Gibbs free energy profile for the decomposition reaction of RO-Cu(Nap)OH and hexane

228x135mm (300 x 300 DPI)

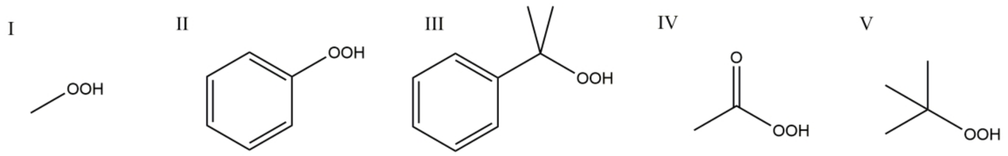

Figure 12. Further peroxide molecules investigated, methyl peroxide (I), phenyl hydroperoxide (II), cumene hydroperoxide (III), peracid (IV) and tert-butylhydroperoxide (V)

215x33mm (300 x 300 DPI)